INTERNATIONAL JOURNAL FOR NUMERICAL METHODS IN FLUIDS
Int. J. Numer. Meth. Fluids 2005; **48**:107–113
Published online 4 March 2005 in Wiley InterScience (www.interscience.wiley.com). DOI: 10.1002/fld.946

Calculation of heat transfer in Ranque–Hilcsh's vortex tube‡

E. L. Tarunin*,† and O. N. Alikina

Perm state university, Bukireva Str. 15, Perm 614099, Russian Federation

SUMMARY

This paper describes problems of calculation of hydrodynamics and heat transfer in vortex tube for *International Journal for Numerical Methods in Fluids*. The Ranque effect has been known since 1931. The existence of the effect is proved by multiple experiments, but there is no strict physical explanation of the effect and there are more than ten hypotheses. Our calculations show that there is no need to use any additional hypothesis to explain the effect, but it is necessary to solve the difficult problem of hydrodynamics of compressible gas in complex geometry. Copyright © 2005 John Wiley & Sons, Ltd.

KEY WORDS: Ranque–Hilsch effect; gas dynamics; CFD modelling; Navier–Stokes equations

1. INTRODUCTION

Vortex effect or Ranque's effect [1, 2] is very well-known phenomenon. It consists in the separation of a rotated gas flux into two parts. One of the fluxes has a temperature that is higher than the entering flux temperature, the other has a lower one. Almost all research done in the area is experimental [3, 4]. At the moment we know several numerical works, devoted to the effect, but amount of dependencies obtained in References [5, 6] is not large. The researchers in laboratories tune the tube using empirical data and intuition [1–4, 7, 8]. By means of mathematical calculation the effect was calculated in Reference [9]. In that work compressibility of the media was taken into account only in the equation of heat transfer. This article is continuation of computational experiments of Reference [9]. Solutions were obtained from full Navier–Stokes' equations with viscosity and temperature conductivity dependence on temperature taken into account. Calculations were carried out in natural

*Correspondence to: E. L. Tarunin, Perm state university, Bukireva Str. 15, Perm 614099, Russian Federation.
†E-mail: evgeny.tarunin@psu.ru
‡This was originally submitted as part of the ICFD SPECIAL ISSUE.

Contract/grant sponsor: Russian Fund of Fundamental Research; contract/grant number: 02-01-96402

Received 27 April 2004
Revised 23 December 2004
Accepted 29 January 2005

variables on a non-uniform mesh until stationary solutions were obtained. Dependencies of the temperature separation effect on different parameters of the vortex tube were obtained and, thus, any doubts about the possibility to describe the effect by gas dynamics were removed.

2. PROBLEM DEFINITION AND SOLUTION PROCEDURE

A vortex cylindrical tube has two outlets. Gas enters the tube usually through by one or two nozzles, placed on the side area of the tube at some angle (so-called angle of inclination). In Figure 1 a countercurrent vortex tube with two rectangular nozzles is presented. In Figure 1 a shortened tube is shown (usually its length is more than 10 diameters). Compressed air creates a flux with high velocity comparable to the sound speed. The flux has an intense rotated flow form. Heated gas goes out of the peripheral annular exit on the opposite side of the tube, and cooled gas is picked at the diaphragm. The diaphragm can be placed on the end of the tube near the nozzles (countercurrent tube) and near the hot exit (direct-flow tube). Flow discharges are adjusted by the throttle, which allows to change the size of the outflow face. The effects of heating and cooling are estimated by average temperature in the entering and outgoing fluxes.

Equations of compressible gas were solved for axially symmetric laminar flow of the ideal gas. The dependencies of viscosity and heat conductivity on temperature were taken into account and viscous dissipation was inserted in energy equation. The equations to be solved

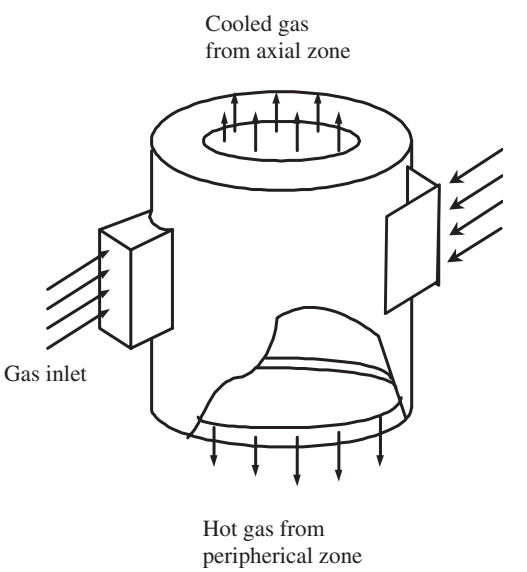

Figure 1. Countercurrent tube.

were as follows [10, 11]:

$$\frac{\partial V_r}{\partial t}+V_r\frac{\partial V_r}{\partial r}+V_z\frac{\partial V_r}{\partial z}-\frac{V_\varphi^2}{r}=-\frac{1}{\rho\gamma^2M^2}\frac{\partial(\rho T)}{\partial r}+\frac{1}{\rho Re}\left(\frac{1}{3}\frac{\partial}{\partial r}(v\,\mathrm{div}\,V)+\frac{\partial}{\partial z}\left(v\frac{\partial V_r}{\partial z}\right)\right.$$
$$+\frac{\partial}{\partial r}\left(v\frac{\partial V_r}{\partial r}\right)+\frac{\partial}{\partial z}\left(v\frac{\partial V_z}{\partial r}\right)-\frac{\partial}{\partial r}\left(v\frac{\partial V_r}{\partial z}\right)$$
$$\left.+\frac{v}{r}\left(\frac{\partial V_r}{\partial r}-\frac{V_r}{r}\right)-\frac{\partial v}{\partial r}\frac{V_r}{r}\right)$$

$$\frac{\partial V_\varphi}{\partial t}+V_r\frac{\partial V_\varphi}{\partial r}+V_z\frac{\partial V_\varphi}{\partial z}+\frac{V_\varphi V_r}{r}=\frac{1}{\rho Re}\frac{\partial}{\partial z}\left(v\frac{\partial V_\varphi}{\partial z}\right)+\frac{\partial}{\partial r}\left(v\frac{\partial V_\varphi}{\partial r}\right)-\frac{1}{r}\frac{\partial}{\partial r}(vV_\varphi)$$

$$\frac{\partial V_z}{\partial t}+V_r\frac{\partial V_z}{\partial r}+V_z\frac{\partial V_z}{\partial z}=-\frac{1}{\rho\gamma^2M^2}\frac{\partial(\rho T)}{\partial z}+\frac{1}{\rho Re}\left(\frac{1}{3}\frac{\partial}{\partial z}(v\,\mathrm{div}\,V)+\frac{\partial}{\partial z}\left(v\frac{\partial V_z}{\partial z}\right)\right.$$
$$+\frac{\partial}{\partial r}\left(v\frac{\partial V_z}{\partial r}\right)+\frac{\partial}{\partial r}\left(v\frac{\partial V_r}{\partial z}\right)$$
$$\left.-\frac{\partial}{\partial z}\left(v\frac{\partial V_r}{\partial r}\right)+\frac{v}{z}\frac{\partial V_z}{\partial r}-\frac{\partial v}{\partial z}\frac{V_r}{r}\right)$$

$$\frac{\partial\rho}{\partial t}+\frac{1}{r}\frac{\partial}{\partial r}(r\rho V_r)+\frac{\partial(\rho V_z)}{\partial z}=0$$

$$\frac{\partial T}{\partial t}+V_r\frac{\partial T}{\partial r}+V_z\frac{\partial T}{\partial z}+(\gamma-1)T\,\mathrm{div}\,V=\frac{\gamma}{RePr}\,\mathrm{div}(\lambda\nabla T)+\frac{M^2}{Re}\gamma(\gamma-1)\Phi$$

$$\Phi=2\left[\left(\frac{\partial V_r}{\partial r}\right)^2+\left(\frac{V_r}{r}\right)^2+\left(\frac{\partial V_z}{\partial z}\right)^2\right]+\left(\left(\frac{\partial V_r}{\partial z}\right)+\left(\frac{\partial V_z}{\partial r}\right)\right)^2+\left(\frac{\partial V_\varphi}{\partial r}-\frac{V_\varphi}{r}\right)$$

Here $V=(V_r,V_z,V_\varphi)$—velocity vector, ρ—density, T—temperature, v—viscosity, $\gamma=C_p/C_V$, Φ—dissipation function.

The assumption about the axial symmetry of the flow makes a three dimensional flux two-dimensional, and thus decreases the amount of computations to feasible. However, we must note, that the experiments [8] distinctly showed that the flow in the tube was not stationary and its vortex structure was not symmetric. In solving this problem we account turbulence by depreciating Reynolds' number (the usage of more accurate turbulent model will be our further research). According to Reference [12], the recommended depreciated Reynolds number equal to 406 has been used. The equations were converted to a non-dimensional form with the following similarity criteria—Reynolds number Re, Mach number M and Prandtl number Pr. The dependence of non-dimensional viscosity on temperature was approximated by Sutherland's formula [11]. A similar dependence was used for the heat conductivity coefficient.

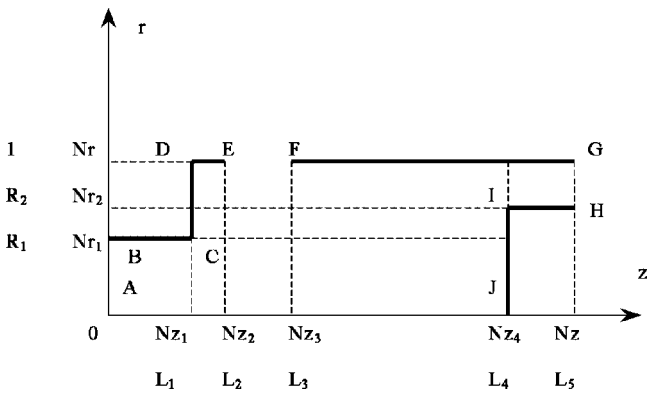

Figure 2. Calculation area with boundary indication and its fragmentation to subareas.

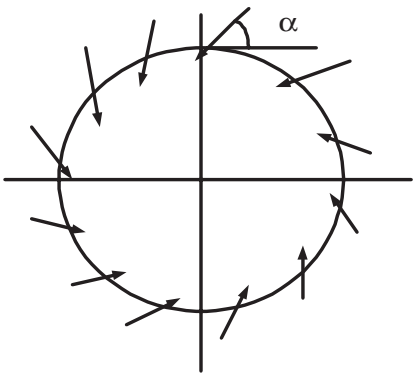

Figure 3. Distribution of entering flux on side area.

The calculation area is represented in Figure 2. At the transition to axially symmetric problem we assumed that the full flux through the inlet should be distributed on the belt EF on the cylindrical surface of the tube. Thus, the velocity of gas on the section of the belt EF must have the radial component connected with full content $Q = V_0 F_c$ through the nozzle by the ratio $V_r = F/F_1$, F—nozzle sectional area, F_1—belt surface area. In dimensionless form we have

$$EF: V_r = -\sin\alpha\cos\beta,\ V_\varphi = \cos\alpha\cos\beta,\ V_z = \sin\beta,\ T = 1,\ \rho = 1$$

Here α is the angle of 'inclination' of the entering flux (Figure 3) and β is the degree of the entering flux rotation. At the outlets we used the following conditions [13] (excluding density):

$$AB, GH: \frac{\partial^2 V_r}{\partial z^2} = 0,\ \frac{\partial^2 V_\varphi}{\partial z^2} = 0,\ \frac{\partial^2 V_z}{\partial z^2} = 0,\ \frac{\partial^2 T}{\partial z^2} = 0,\ \rho = \frac{1}{\Delta PT}$$

Here ΔP is assigned pressure drop (the ratio of pressure at the inlet to that at the outlet of the vortex tube). Let us note, that we assume the equality of pressures at the outlets of the vortex tube in order to decrease of parameters number. On the solid boundaries it is assumed: $V=0,\ \partial T/\partial n=0,\ \partial\rho/\partial n=0$. Such assignment of boundary conditions for the temperature on the tube solid boundaries corresponds to so-called 'adiabatic' vortex tube [7]. On the axis the symmetry condition is applied. Problem solving starts from applying initial conditions and problem parameters. Inside the calculation area homogeneous initial conditions are applied for velocity components and temperature $V=0,\ T=1$ and the initial distribution of density field is obtained from the mixed problem for Laplace equation inside the area:

$$\Delta\rho=0,\ G:\frac{\partial\rho}{\partial n}=0,\ EF:\rho=1,AB,\ GH:\rho=\frac{1}{\Delta P}$$

Here G is a solid part of the tube. Such distribution for density forms a flux that is close to real. The problem was solved by a finite differences method. We used an explicit scheme with upwind approximation (for convective components) [13, 14]. In evolutionary equations we lifted all the components that could perfect the stability of the scheme to the upper $(n+1)$th layer. We used a nonuniform mesh to be able to decrease computational viscosity and to continuously change the geometrical parameters. Equations were iterated to stationary state. For example, the discrepancy of the values dropped ten times by 5000 iteration for 13000 mesh points.

3. COMPUTATIONAL RESULTS

The main results were obtained for the following set of parameters $Re=150$–$450,\ \gamma=1.4,\ \alpha=0.05$–$0.20,\ \beta=\pi/5,\ M=0.8$–$1.0,\ R_1=0.2$–$0.5,\ R_2=0.7$–$0.8,\ \Delta P=2,\ L_1=0.5,\ L_2=0.7,\ L_3=1.0,\ L_4=2.5$–$4.2,\ L_5=2.8$–$4.5$. One of the most important parameter in the above list is assigned pressure drop ΔP. We have to show the relation of this parameters to the real pressure drop. It is natural to assume, that rest gas transforms to the entering flux with assigned velocity V_0 by adiabatic process. It makes the full pressure drop equal to:

$$\tilde{k}=\frac{p_0}{p_{\text{ent}}}=\frac{p_0}{p_1}\Delta P=\left(1+\frac{\gamma-1}{2}M^2\right)\Delta P$$

This formula shows that at the Mach number equal to 0.8 and $\gamma=1.4$ the real value of drop pressure is 1.5024 times more than that assigned in the list of parameters. Flow lines are shown in Figure 4. The axis are marked by mesh points. The main feature of the flow is the vortex zone of the recurrent flow, the existence of which was doubted in many papers [3]. The estimation of the values shows, that numerical viscosity is not low. The decrease in the numerical viscosity (Reynolds number $Re_h<1$) can be achieved only by noticeable increase of computational time. The dependence of the temperatures difference on the Reynolds number is shown in Figure 5. The maximum temperature difference varied from 0.35 to 1.01 (in dimension form it is about 100 and 270°).

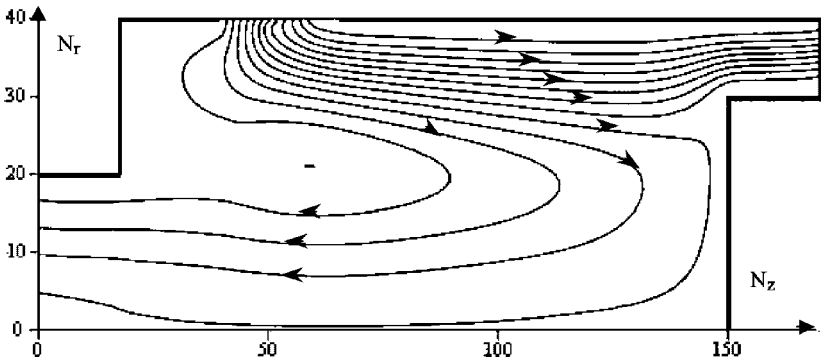

Figure 4. Flow lines.

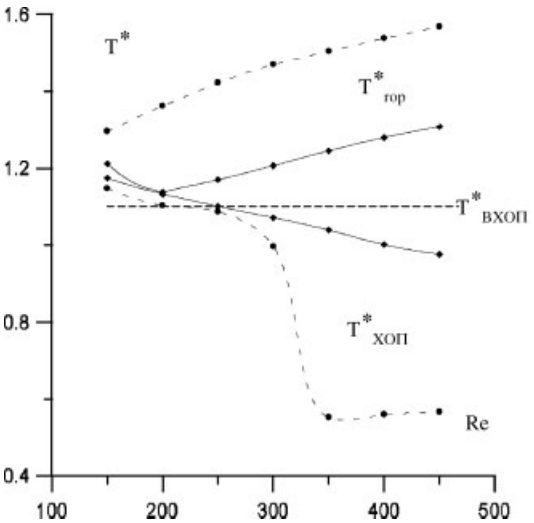

Figure 5. Dependence of stagnation temperature T^* on Reynolds number Re.

4. CONCLUSIONS

The influence of problem parameters and geometrical parameters on calculating values has been studied. The dependencies of the main characteristics have been obtained on different parameters of the tube (length of the tube, inclination angle of entering flux, degree of rotation of entering flux, Reynolds and Mach numbers, radii of diaphragm and throttle and etc.). The main result is that we can describe the process in the vortex tube by ordinary gas dynamics without using any additional hypothesis.

REFERENCES

1. Ranque GJ. *Journal de Physique et la Radium* 1933; **7**(4):112–115.
2. Hilcsh R. Die Expansion von Gasen in Zentrifugalfeldes als Kalte prozes. *Zeitschrift fur Naturforschung* 1946; **1**:208–214.

3. Gutsol AF. Vortex effect. *Journal of Physical Successes* 1997; **167**(6):665–687.
4. Piralishvili ShA *et al.* Vortex effect. *Experiments*, *Theory and Technical Solutions*. Energomash: Moscow, 2000; 412.
5. Bezprozvannykh V *et al.* The Ranque–Hilsch effect. CFD modelling. *Proceedings of International Conference on Advanced problems in Thermal Convection*, Perm, 2003.
6. Skovorodko PA. Simulation of the flow in Ranque–Hilsch tube. *Nauchnye Itogi-98*, Novosibirsk, 1999; 11–12.
7. Merculov AP. Vortex effect and its application in technics. *Engineering*. Mashinostroenie: Moscow, 1969.
8. Arbusov VA *et al.* Observation of large-scale hydrodynamics structures in vortex tube and Ranque's effect. *Letters to Journal of Thermal Physics* 1997; **23**(23):84–90.
9. Lubimov DV *et al.* The theoretical model of Ranque's effect. *Scientific Journal of Mathematica* 1994; (1): 162–177.
10. Landau LD, Lifshits EM. Theoretical physics. *Hydrodynamics*, vol. 6. Nauka: Moscow, 1986.
11. Rachmatulin HA. *Gas Dynamics*. Moscow High School Publishers: Moscow, 1965; 723.
12. Rochino L. Analitical researches of incompressible turbulent rotated flux in stationary tubes. *American Society of Mechanical Engineers Proceedings*, vol. 2, E. Moscow, 1969; 2–16.
13. Rouch P. *Computational Hydrodynamics*. Moscow Mir Publishers: Moscow, 1980.
14. Tarunin EL. *Computational Experiments in Problems of Free Convection*. Irkutsk University Publishers: Irkutsk, 1990; 226.

